

# Thermal and Elastic Effects upon Crystallization of the Metallic Glass Pd<sub>40</sub>Cu<sub>30</sub>Ni<sub>10</sub>P<sub>20</sub>

N. P. Kobelev<sup>a</sup>, V. A. Khonik<sup>b</sup>, and G. V. Afonin<sup>b,\*</sup>

<sup>a</sup> *Institute of Solid State Physics, Russian Academy of Sciences,  
ul. Akademika Ossipyana 2, Chernogolovka, Moscow oblast, 142432 Russia*

<sup>b</sup> *Voronezh State Pedagogical University, ul. Lenina 86, Voronezh, 394043 Russia*

\* e-mail: [afoningv@gmail.com](mailto:afoningv@gmail.com)

Received March 31, 2015

**Abstract**—The change in the shear modulus upon crystallization and the heat of crystallization of the bulk metallic glass Pd<sub>40</sub>Cu<sub>30</sub>Ni<sub>10</sub>P<sub>20</sub> have been determined. It has been shown that the obtained results can be explained in terms of the model assuming the existence of “defects” in the glass structure, which are similar to elastic dipoles in crystals.

**DOI:** 10.1134/S1063783415090176

## 1. INTRODUCTION

Although thermal and elastic effects during heat treatment of metallic glasses were already observed at the earliest stages of their studies and they were studied in many works [1–7], concrete mechanisms of realizing these effects are discussable up to now. This is due to insufficient understanding the nature of formation of the structure and, correspondingly, mechanisms determining specific features of the physical properties of metallic glasses. Foregoing can be referred to both processes proceeding in metallic glasses at temperatures lower than the crystallization temperature (i.e., to so-called structural relaxation) and processes proceeding during their crystallization.

A unified approach to these phenomena was proposed in the interstitial theory of condensed state by Granato [8, 9] that determines the genetic bond between properties of a crystal, the liquid, and the glass. This bond is based on the hypothesis that the melting of simple metals is due to fast generation of interstitial atoms in a split (dumbbell-like) configuration in the crystal structure, which sharply decreases the shear modulus (loss of the shear stability) of a material and can be interpreted as melting [10]. The formation of a metallic glass structure is related to “freezing” of significant concentrations of interstitial dumbbells during melt quenching. The Granato model allowed the qualitative and quantitative explanation of fairly many phenomena observed in liquid and solid amorphous states [11–13].

In [14], we proposed a new approach to the problem of formation and evolution of the properties of metallic glasses that is based, to a significant degree, on the Granato theory ideology and permits its

extension to multicomponent systems. This approach is based on the fact that a split interstitial site is a special case of an “elastic dipole,” i.e., an atomic configuration with a local symmetry that is lower than that of the surrounding matrix [15]. Such “defect” can be identified in a macroscopically isotropic material like a metallic glass. The assumption that the glass structure contains “defects” such as elastic dipoles made it possible to deduce simple expressions for the internal energy and the elastic characteristics of the glass and to demonstrate a direct correlation between thermal effects and the change in the elastic characteristics during the structural relaxation of metallic glasses confirmed experimentally [14]. In [16], these expressions were examined for the case of thermal and elastic effects during crystallization of bulk metallic glass Zr<sub>52.5</sub>Ti<sub>5</sub>Cu<sub>17.9</sub>Ni<sub>14.6</sub>Al<sub>10</sub> and a good agreement was found between the calculations and the experiment.

In this work, we continue the studies of the thermal and the elastic effects that take place during crystallization of bulk metallic glass Pd<sub>40</sub>Cu<sub>30</sub>Ni<sub>10</sub>P<sub>20</sub>.

## 2. BASIC RELATIONSHIPS

Basic relationships for the internal energy and the elastic characteristics of a metallic glass is based on the hypothesis that its structure contains “defects” like elastic dipoles which cause additional internal strains  $\varepsilon_{ij}$  and, correspondingly, increase the internal energy.

Since a metallic glass is macroscopically isotropic, the change in the internal energy  $\Delta U$  can be written as

an expansion with respect to invariants of the internal strain [14, 16]

$$\rho_0 \Delta U = \frac{\lambda}{2} I_1^2 + \mu I_2 + \frac{\nu_1}{6} I_1^3 + \nu_2 I_1 I_2 + \frac{4}{3} \nu_3 I_3 + \frac{1}{24} \gamma_1 I_1^4 + \frac{1}{2} \gamma_2 I_1^2 I_2 + \frac{4}{3} \gamma_3 I_1 I_3 + \frac{1}{2} \gamma_4 I_2^2 + \dots, \quad (1)$$

where  $\rho_0$  is the density,  $\lambda$  and  $\mu$  are the second-order Lamé constants,  $\nu_\alpha$  and  $\gamma_\beta$  ( $\alpha = 1-3$ ,  $\beta = 1-4$ ) are the third-order and the fourth-order Lamé constants of the mother crystal, respectively;  $I_1 = \varepsilon_{ii}$ ,  $I_2 = \varepsilon_{ij} \varepsilon_{ji}$ , and  $I_3 = \varepsilon_{ij} \varepsilon_{jk} \varepsilon_{ki}$  are the strain matrix invariants. Because elastic dipoles interact to an external stress, they can be characterized by the tensor of the second rank [15]

$$\lambda_{ij} = \frac{\partial}{\partial c} \int \varepsilon_{ij}^0 dV \quad (2)$$

whose components are equal to the components of the strain tensor  $\varepsilon_{ij}^0$  per unit of concentration  $c$  of elastic dipoles created by a field of one-direction dipoles ( $V$  is the material volume). Similarly, the tensor of the fourth rank can be introduced [14, 16]

$$\lambda_{ij} \lambda_{kl} = \frac{\partial}{\partial c} \int \varepsilon_{ij}^0 \varepsilon_{kl}^0 dV, \quad (3)$$

that also characterizes the elastic parameters of a dipole. It is easy to note that  $\lambda_{ij}$  and  $\lambda_{ij} \lambda_{ji}$  are invariants of the elastic field of a dipole. It was shown [14, 16] that, during heat treatment of a metallic glass, the dilatation effects (changes in volume) give a negligible contribution to thermal effects and changes in the elastic characteristics in the region of structural relaxation and during crystallization of the glass. This is must be all the more valid for the  $\text{Pd}_{40}\text{Cu}_{30}\text{Ni}_{10}\text{P}_{20}$  alloy, since the change in its density is almost an order lower [17, 18] than that in other metallic glasses. In this case, we can neglect terms with  $I_1$  in Eq. (1) and, restricting our consideration only by first terms of the expansion, obtain the following expressions for the internal energy and effective shear modulus  $G$  of a metallic glass based on Eqs. (1)–(3) [14, 16]:

$$\rho_0 \Delta U \approx \mu c \langle \lambda_{ij} \lambda_{ji} \rangle, \quad (4)$$

$$G \approx \mu + \gamma_4 \Omega_r c \langle \lambda_{ij} \lambda_{ji} \rangle, \quad (5)$$

where  $\Omega_r \sim 1.38$  is the averaged value of the form-factor (that takes into account various types of dipoles) for the shear strain [14]. As seen from Eqs. (4) and (5), there must be a direct correlation between the changes in the internal energy and the shear modulus of a glass. For example, during crystallization when elastic dipoles “frozen” into the structure of a metallic glass disappear, the relationship

$$G - \mu = \frac{\gamma_4 \Omega_r}{\mu} \rho_0 \Delta U \quad (6)$$

must be fulfilled.

### 3. EXPERIMENTAL TECHNIQUE

As follows from Eq. (6), its numerical verification needs the knowledge of nonlinear elasticity modulus  $\gamma_4$  that reflects anharmonicity of the interatomic interaction. Up to now, this parameter was only known for the  $\text{Zr}_{52.5}\text{Ti}_5\text{Cu}_{17.9}\text{Ni}_{14.6}\text{Al}_{10}$  glass [19]. However, analogous data [20] were recently obtained for the  $\text{Pd}_{40}\text{Cu}_{30}\text{Ni}_{10}\text{P}_{20}$  glass, and this is the reason why exactly this material was chosen to perform this study (as far as we know, this is the second composition of metallic glasses for which the fourth-order elastic moduli were determined).

The elastic characteristics were found by an acoustic method from the measurements of the sound velocities by the echo–pulse method in the transmission scheme at a frequency of 5 MHz [21]. The noncrystallinity of the initial glasses was controlled by X-ray diffraction. Samples for measurements of the sound velocity have sizes  $\sim 3 \times 6 \times 15$  mm. The samples were heat-treated by heating to a given temperature at a rate of 5 K/min with subsequent cooling at a rate of 5–10 K/min. The thermal effects were measured by differential scanning calorimetry (DSC) using a Hitachi Exstar DSC7020 calorimeter in an argon flow. The characteristic mass of the samples was  $\sim 40$  mg. The measurements were carried out at a heating rate of 5 K/min.

### 4. RESULTS AND DISCUSSION

Shear-wave velocity  $V_t$  in samples of the  $\text{Pd}_{40}\text{Cu}_{30}\text{Ni}_{10}\text{P}_{20}$  metallic glass was  $(1.935 \pm 0.005) \times 10^3$  m/s in the initial state at room temperature, and  $(1.963 \pm 0.002) \times 10^3$  m/s in the relaxed state (after heating to the vitrification temperature 565 K. In the same samples, after crystallization as a result of heating to 673 and 773 K,  $V_t = (2.0650 \pm 0.005) \times 10^3$  m/s and  $(2.230 \pm 0.005) \times 10^3$  m/s, respectively. The measured transverse sound velocities are very close to those found in [18] after annealing at corresponding temperatures. Relationship (6) was verified using the value of the shear modulus measured in relaxed samples of the metallic glass as the basis value. The reason is that the parameters of the glass in the initial state (immediately after melt quenching) can noticeably vary in dependence of the quenching conditions. In addition, the higher-order moduli were measured in [20] exactly for the relaxed state. Thus, the change in the shear modulus of the alloy was  $3.8 \pm 0.2$  GPa at the first crystallization stage and  $10.3 \pm 0.2$  GPa after the second crystallization (here, the material density in the relaxed state was taken to be  $9.3$  g/cm<sup>3</sup>).

The heat of crystallization was determined using DSC measurements. The measurement scheme was as follows. During the first cycle, the sample was heated

to the vitrification temperature and, then, cooled to room temperature at almost the same rate to obtain a relaxed state. During the second cycle, the sample was heated to a temperature higher than the crystallization temperature (to 673 or 773 K). During the third cycle, the sample was repeatedly heated to the same temperature. In two latter cycles, we measured heat flow  $W$ . The thermal effect was calculated as

$$Q = \frac{1}{\dot{T}} \int_{T_R}^T (W_2 - W_3) dT, \quad (7)$$

where  $T_R$  is room temperature and  $\dot{T}$  is the heating rate. In a number of cases, we performed the fourth cycle of the measurements, whose results demonstrated the coincidence of values  $W_3(T)$  and  $W_4(T)$  within the measurement accuracy.

Figure depicts the temperature dependences of the difference heat flow and the magnitudes of the thermal effect on heating to 673 and 773 K. After heating above the first (main) crystallization peak, the crystallization heat was  $36.5 \pm 2$  J/g or  $0.34$  J/m<sup>3</sup> (at  $\rho = 9.3$  g/cm<sup>3</sup>). The shear modulus of the samples crystallized at 673 K is  $39.65 \pm 0.2$  GPa, according to the data of measuring shear vibrations. The calculation by Eq. (6) using this value gives  $\gamma_4 = -320 \pm 30$  GPa that almost coincides with the value  $\gamma_4 = -300 \pm 40$  GPa, obtained in [20].

At the same time, similar estimation obtained on the base of comparison the shear moduli in the relaxed state and the state crystallized at 773 K ( $\sim 46.2$  GPa) and the thermal effect of  $40 \pm 2$  J/g during heating to this temperature gives  $\gamma_4 \sim -930$  GPa, i.e., the value that is almost 3 times higher in magnitude. In this case, we call attention to the fact that the fairly significant change in the effective shear modulus during the second crystallization stage (almost by 6.5 GPa) is accompanied by very insignificant increase in the summary thermal effect. This is thought can be related to the fact that the second (low) peak in the DSC curve is not immediately related to the crystallization process (i.e., annihilation of elastic dipoles in terms of the approach under consideration). As follows from the data of [18], at temperatures higher than 680–690 K, the Pd<sub>2</sub>Cu<sub>2</sub>P-type phase starts to form; the phase was not observed in the structure after the first crystallization stage. Because of this, the sharp increase in the shear modulus is most likely due to a phase transition (formation of a new phase having higher elastic characteristics). At the same time, the internal energy of this phase is likely close in magnitude to the energies of the phases formed at the first crystallization stage, and this is the cause why the thermal effect has a small magnitude.

Thus, it can be suggested that the annihilation of the elastic dipoles, in terms of the model under consideration, occurs in the Pd<sub>40</sub>Cu<sub>30</sub>Ni<sub>10</sub>P<sub>20</sub> alloy at the first (main) stage of its crystallization. Parameters of

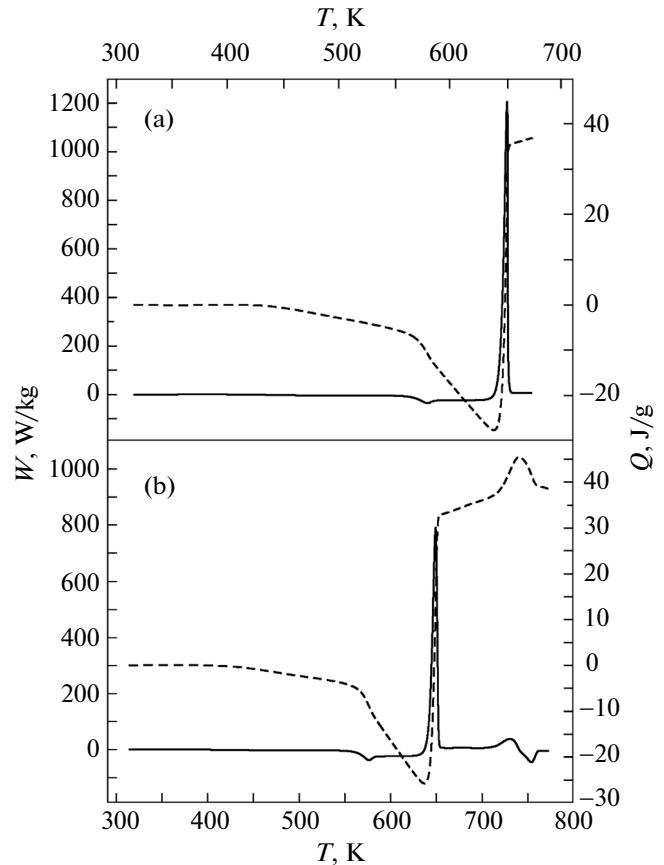


**Fig. 1.** Thermal effects induced upon heating of the bulk metallic glass Pd<sub>40</sub>Cu<sub>30</sub>Ni<sub>10</sub>P<sub>20</sub> to temperatures of (a) 673 and (b) 773 K. The solid line shows the differential heat flow  $W(T)$ , and the dashed line indicates the summary thermal effect  $Q(T)$  calculated by Eq. (7).

these elastic dipoles can be approximately estimated using, for example, Eq. (5). Assuming, according to [8, 16], that their concentration in the metallic glass must be of  $\sim 3\%$ , we obtain  $\lambda_{ij}\lambda_{ji} \approx 0.3$ , that is within the limits of characteristic values of this parameter for elastic dipoles in simple crystalline metals [15]. Underline once again that the change in the internal energy and in the shear modulus during structural transformations of the glass are substantially anharmonic phenomena.

## 5. CONCLUSIONS

The studies performed in this work show that the model based on the assumption that the structure of the metallic glass contains “defects” similar to elastic dipoles in the crystals makes it possible to properly estimate the decrease in the shear modulus of the glass as compared to that of the mother crystal and the value of the thermal effects during the glass crystallization. The relationships between the internal energy and the effective shear modulus of the metallic glass obtained based on this model agree with the changes in these

characteristics observed experimentally during the glass crystallization.

#### ACKNOWLEDGMENTS

This study was supported by the Ministry of Education and Science of the Russian Federation (task no. 3.114.2014/K for the study in the framework of the project part of the State Task for scientific researches).

#### REFERENCES

1. H. S. Chen and D. Turnbull, *J. Chem. Phys.* **48**, 2560 (1968).
2. H. S. Chen and T. T. Wang, *J. Appl. Phys.* **41**, 5338 (1970).
3. T. Masumoto and R. Maddin, *Acta Metall.* **19**, 725 (1971).
4. J. Logan and M. F. Ashby, *Acta Metall.* **22**, 1047 (1974).
5. D. J. Safarik and R. B. Schwarz, *Acta Mater.* **55**, 5736 (2007).
6. C. A. Schuh, T. C. Hufnagel, and U. Ramamurty, *Acta Mater.* **55**, 4067 (2007).
7. T. Egami, T. Iwashita, and W. Dmowski, *Metals* **3**, 77 (2013).
8. A. V. Granato, *Phys. Rev. Lett.* **68**, 974 (1992).
9. A. V. Granato, *Eur. Phys. J. B* **87**, 18 (2014).
10. M. Born, *J. Chem. Phys.* **7**, 591 (1939).
11. A. V. Granato, D. M. Joncich, and V. A. Khonik, *Appl. Phys. Lett.* **97**, 171911 (2010).
12. A. S. Makarov, V. A. Khonik, Yu. P. Mitrofanov, A. V. Granato, D. M. Joncich, and S. V. Khonik, *Appl. Phys. Lett.* **102**, 091908 (2013).
13. V. A. Khonik and N. P. Kobelev, *J. Appl. Phys.* **115**, 093510 (2014).
14. N. P. Kobelev, V. A. Khonik, A. S. Makarov, G. V. Afonin, and Yu. P. Mitrofanov, *J. Appl. Phys.* **115**, 033513 (2014).
15. A. S. Nowick and B. S. Berry, *Anelastic Relaxation in Crystalline Solids* (Academic, London, 1972; Atomizdat, Moscow, 1975).
16. N. P. Kobelev, V. A. Khonik, G. V. Afonin, and E. L. Kolyvanov, *J. Non-Cryst. Solids* **411**, 1 (2015).
17. T. D. Shen, U. Harms, and R. B. Schwarz, *Appl. Phys. Lett.* **87**, 4512 (2003).
18. G. E. Abrosimova, N. S. Afonikova, N. P. Kobelev, E. L. Kolyvanov, and V. A. Khonik, *Phys. Solid State* **49** (11), 2099 (2007).
19. N. P. Kobelev, E. L. Kolyvanov, and V. A. Khonik, *Phys. Solid State* **49** (7), 1209 (2007).
20. N. P. Kobelev, E. L. Kolyvanov, and V. A. Khonik, *Phys. Solid State* **57** (2015) (in press).
21. N. P. Kobelev, R. K. Nikolaev, Ya. M. Soifer, and S. S. Khasanov, *Phys. Solid State* **40** (1), 154 (1998).

*Translated by Yu. Ryzhkov*